# Chapter 3
Grain Boundary Control to Obtain Heat-Resistant Silicon Nitride

3.1 Addition of Yb_2O_3 and Lu_2O_3 to Silicon Nitride Ceramics as Sintering Additives

Silicon nitride ceramics are composed of silicon nitride grains and a grain boundary phase, as mentioned in Sect. 1.1. The grain boundary phase softens and/or becomes a mass transfer path at high temperatures. The formation of a heat-resistant grain boundary phase is necessary for to obtain heat-resistant silicon nitride ceramics, which means that control of the addition of sintering additives is important.

Yttrium oxide (Y_2O_3) is added as a sintering additive to obtain heat-resistant silicon nitride ceramics [1]. When Y_2O_3 and SiO_2 are added together, yttrium silicates, Y_2SiO_5 and $Y_2Si_2O_7$, which have high melting temperatures, are crystallized at multigrain junctions by heat treatment after sintering. Although such crystallization is effective for improving the heat resistance of silicon nitride ceramics, decreased strength and heat resistance have been reported. Probable reasons for the degradation are the existence of an amorphous layer between the crystalline silicate phase and the silicon nitride grains, and residual stress induced by the difference in thermal expansion between the silicates and silicon nitride [2]. These results suggest that the silicates are not effective for improving the heat resistance of silicon nitride ceramics. Various rare-earth silicon oxynitrides exist with the phase relationship RE_2O_3–SiO_2–Si_3N_4 (RE: Sc, Y, and rare-earth elements) (Fig. 3.1). Among the oxynitrides, $RE_4Si_2O_7N_2$-type and $RE_2Si_3O_3N_4$-type oxynitrides have high melting temperatures [3] and their chemical composition is closer to that of silicon nitride (Si_3N_4) than silicates because they contain nitrogen (N). They are thus expected to be effective additives to promote the growth of a crystalline grain boundary phase to achieve heat-resistant silicon nitride. The crystallization of $Y_2Si_3O_3N_4$ was reported by Tsuge et al., but the formation of $Y_2Si_3O_3N_4$, which lies on the tie line between Y_2O_3 and Si_3N_4, in the phase diagram of Y_2O_3–SiO_2–Si_3N_4 is difficult, because SiO_2 always exists on the surface of Si_3N_4 particles [4]. $Y_4Si_2O_7N_2$ cannot coexist with silicon nitride under the
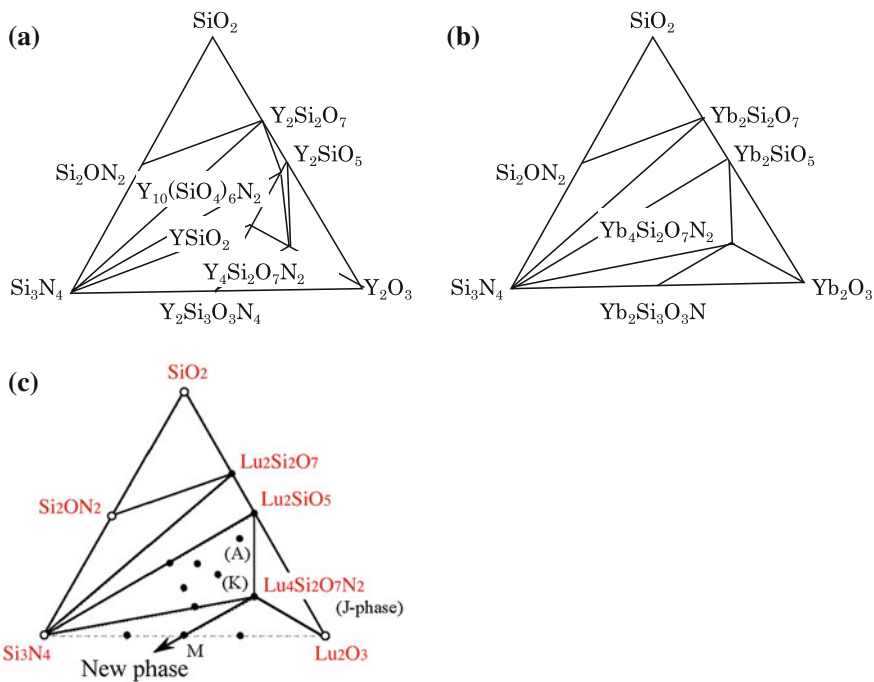
Fig. 3.1 Phase diagrams among Si_3N_4–SiO_2–Y_2O_3 (**a**), Si_3N_4–SiO_2–Yb_2O_3 (**b**), and Si_3N_4–SiO_2–Lu_2O_3 (**c**)

equilibrium state, as shown in the phase diagram of Y_2O_3–SiO_2–Si_3N_4 (Fig. 3.1a) [5]. $Yb_4Si_2O_7N_2$ and $Lu_4Si_2O_7N_2$ can coexist with Si_3N_4 from the phase diagram relationships of Yb_2O_3–SiO_2–Si_3N_4 (Fig. 3.1b) [3] and Lu_2O_3–SiO_2–Si_3N_4 (Fig. 3.1c) [6]. A To investigate the effect of additives on the properties of silicon nitride ceramics, a silicon nitride ceramic including $Yb_4Si_2O_7N_2$ and silicon nitride ceramics including $Lu_4Si_2O_7N_2$ were synthesized and their high-temperature mechanical properties were measured.

3.2 Sintering of Silicon Nitride Ceramics

A silicon nitride powder, RE_2O_3 powder (RE:Yb or Lu), and SiO_2 powder were weighed and mixed in n-hexane by planetary milling using a silicon nitride pot and balls. The mixed powders were hot-pressed in a flow of nitrogen gas for Yb addition or at a nitrogen pressure of 1 MPa for Lu addition under a compressive load. Figure 3.2 shows the shrinkage of the Si_3N_4–$Yb_4Si_2O_7N_2$ powder during hot pressing. Densification curves of the powder, which consists of of 94.1 mol% Si_3N_4, 4.7 mol% Yb_2O_3, and 1.2 mol% SiO_2, are shown in the figure. The powder densified gradually from 1550 °C, rapidly above 1650 °C, and even more rapidly until the middle of the soaking time at 1750 °C [7].

Fig. 3.2 Densification of Si_3N_4 ceramic containing 4.7 mol% Yb_2O_3 and 1.2 mol% SiO_2 during hot pressing [7]
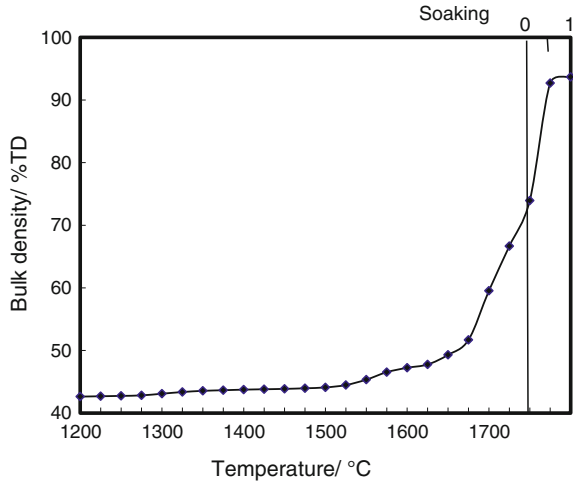
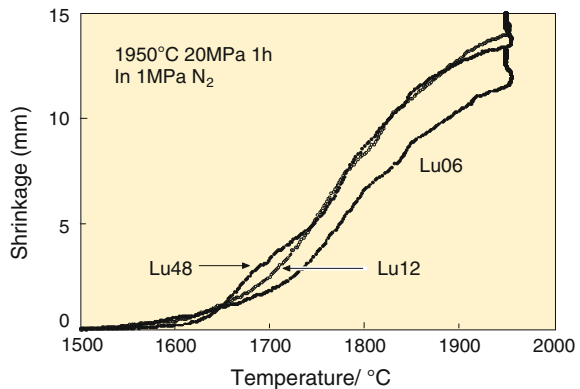**Fig. 3.3** Densification of silicon nitride ceramics with 0.6, 1.2, and 4.8 mol% Lu_2O_3 during hot pressing

Figure 3.3 shows the shrinkage of Si_3N_4–$Lu_4Si_2O_7N_2$ ceramics during hot pressing. Densification starts at about 1570 °C, regardless of the additive content. The ceramics containing 1.2 and 4.8 mol% Lu_2O_3 (Lu12 and Lu48, respectively) were almost completely densified, although the ceramic with 0.6 mol% Lu_2O_3 (Lu06) was not densified after heating to 1950 °C for 1 h.

3.3 High-Temperature Strength of Silicon Nitride Ceramics

The dependence of the bending strength of silicon nitride ceramics with $Yb_4Si_2O_7N_2$ on the temperature is shown in Fig. 3.4 along with the results of previous investigations [2, 8, 9]. The bending strength was 977 MPa at room temperature (RT) and decreased slightly with increasing temperature up to 1350 °C.

Fig. 3.4 High-temperature
bending strength of silicon
nitride with $Yb_4Si_2O_7N_2$. The
bending strengths of silicon
nitride with ytterbium silicates
in previous reports are also
plotted [2, 8, 9]
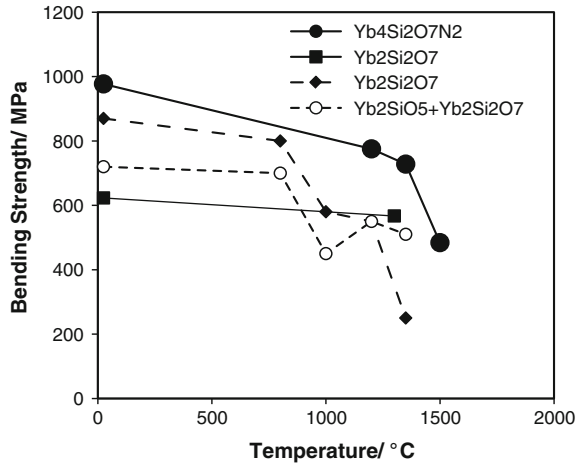
Fig. 3.5 Load-displacement
curves of silicon nitride with
$Yb_4Si_2O_7N_2$ obtained in
bending strength test [9]
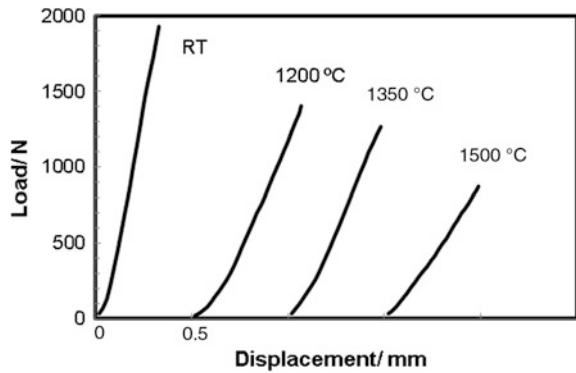
The strength at 1350 °C of 728 MPa is about 75 % of that at RT. The strength was
484 MPa at 1500 °C. Smith and Quackenbush reported the strengths of hot-pressed
silicon nitride ceramics containing Y_2O_3; the strengths of silicon nitride including
6 mass% of Y_2O_3 and 13 mass% of Y_2O_3 at 1500 °C were 380 and 500 MPa,
respectively [10], comparable with our data. The load-displacement curves obtained
in the bending strength test at 1200, 1350, and 1500 °C are shown in Fig. 3.5. The
load-displacement curve is almost straight, indicating no yielding before fracture,
which suggests that the fracture was brittle at each temperature. A report on the
effect of oxides added to gas-pressure-sintered silicon nitride showed that adding
Nd_2O_3 or La_2O_3 together with Y_2O_3 was more effective in increasing the
high-temperature strength than adding MgO or Al_2O_3 together with Y_2O_3. The
load-displacement curves for the materials including Nd_2O_3 and Y_2O_3 at 1200 and
1350 °C indicated brittle fracture, and the degradation of strength and yielding were
clearly observed at 1500 °C.

Fig. 3.6 High-temperature strength of silicon nitride ceramics with 1.2 mol% Lu$_2$O$_3$ (12Lu) and 4.8 mol% Lu$_2$O$_3$ (48Lu) [11]
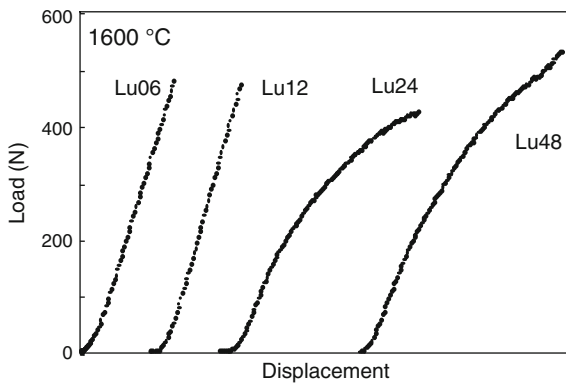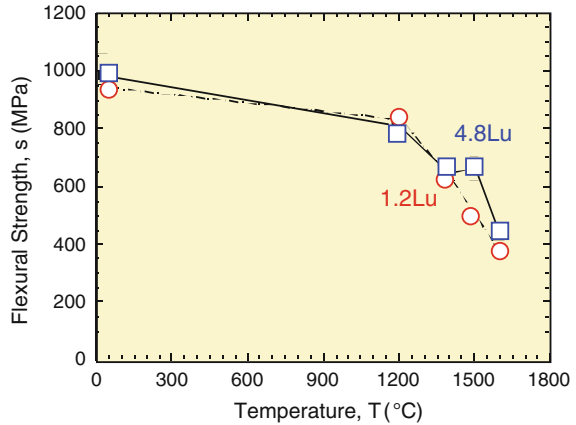
Fig. 3.7 Load-displacement curves of silicon nitride ceramics sintered with Lu$_2$O$_3$ obtained in bending test at 1600 °C. Lu06, Lu12, Lu24, and Lu48 indicate the load-displacement curves for silicon nitride with 0.6, 1.2, 2.4, and 4.8 mol% Lu$_2$O$_3$, respectively

The strength of the Si$_3$N$_4$ ceramic with 1.2 mol% Lu$_2$O$_3$ added was about 1 GPa at RT, which decreased gradually up to 1200 °C, then decreased sharply up to 1600 °C. The strength of the Si$_3$N$_4$ ceramic with 4.8 mol% Lu$_2$O$_3$ added Si$_3$N$_4$ ceramics changed in a similar manner but the strength at 1350 °C was the same as that at 1500 °C. The strength at 1600 °C was 400 MPa for the ceramic with 1.2 mol% Lu$_2$O$_3$ added and 450 MPa for the ceramic with 4.8 mol% Lu$_2$O$_3$ added (Fig. 3.6). This result suggests that the Si$_3$N$_4$ ceramic including 4.8 mol% Lu$_2$O$_3$ is more heat resistant than the Si$_3$N$_4$ ceramic including 1.2 mol% Lu$_2$O$_3$ [11].

Figure 3.7 shows the load-displacement relationships obtained from a bending test carried out on Si$_3$N$_4$ ceramics with different amounts of added Lu$_2$O$_3$ at 1600 °C.

The load-displacement curve of the ceramic with 1.2 mol% Lu_2O_3 is almost straight, but that of the ceramic with 4.8 mol% Lu_2O_3 is convex, indicating that it deformed plastically before fracture. These materials can be used up to the stress at which plastic deformation starts, which is much lower than the apparent strength. Figures 3.6 and 3.7 suggest that the ceramic with 1.2 mol% Lu_2O_3 is more heat resistant than that with 4.8 mol% Lu_2O_3, although the apparent strength of the ceramic with 4.8 mol% Lu_2O_3 is higher than that of the ceramic with 1.2 mol% Lu_2O_3.

3.4 High-Temperature Creep of Silicon Nitride Ceramics

Tensile creep tests were conducted on a silicon nitride ceramic containing Yb_2O_3 and on silicon nitride ceramics containing Lu_2O_3. The silicon nitride ceramic with Yb_2O_3 was fabricated from a powder mixture of 97.6 mol% α-Si_3N_4 and 2.4 mol% $Yb_4Si_2O_7N_2$ (denoted as Yb) by sintering at 1750 °C for 1 h under compression of 20 MPa in nitrogen gas at a pressure of 0.925 MPa. The silicon nitride ceramics with Lu_2O_3 consisted of 95.2 mol% Si_3N_4 and 4.8 mol% Lu_2O_3 (denoted as Lu48) and 98.8 mol% Si_3N_4 with 1.2 mol% Lu_2O_3 (designated as Lu12). Both ceramics were sintered at 1950 °C for 1 h undercompression of 20 MPa in nitrogen gas at a pressure of 1 MPa. Tensile creep tests were then conducted at 1400 and 1500 °C in air. Figure 3.8 shows the results of the tensile creep test at 1500 °C for the silicon nitride ceramic with 4.8 mol% Lu_2O_3 (Lu48). The curves are typical for silicon nitride ceramics, i.e., transient creep was followed by steady-state creep but the

Fig. 3.8 Typical creep curves of silicon nitride with 4.8 mol% Lu_2O_3 (Lu48) at 1500 °C [12]
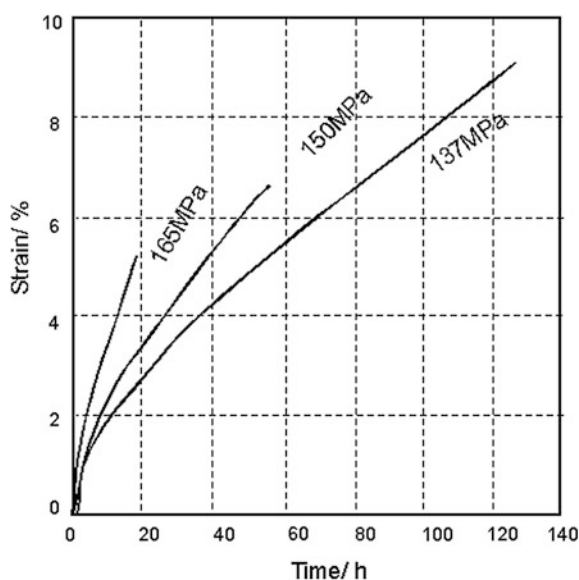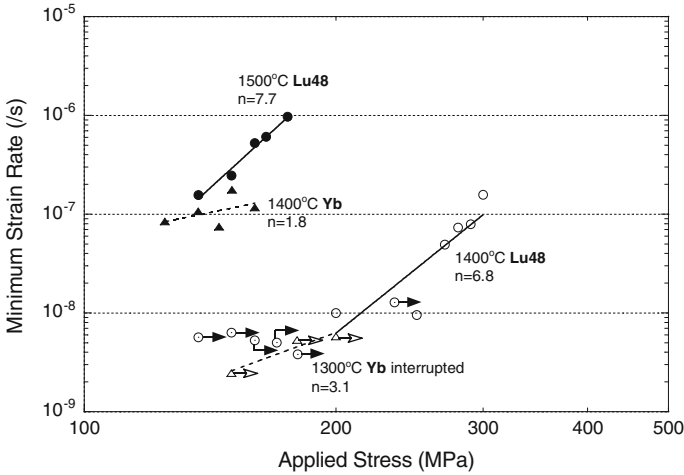
Fig. 3.9 Time to failure and strain rate for Lu48 and Yb at 1400 and 1500 °C [12]

tertiary stage was not observed. The creep rate increases with increasing applied stress [12].

According to Norton's law, the creep rate in the steady state, $\dot{\varepsilon}$, is expressed as a power function of stress σ as follows:

$$\dot{\varepsilon} = D_0 \exp\left(-\frac{Q}{RT}\right)\sigma^n \qquad (3.1)$$

where n is the stress exponent, R is the gas constant, T is the absolute temperature, and Q is the activation energy. The relationship between the minimum strain rate and the applied stress for Lu48, together with the data for silicon nitride sintered with 2.4 mol% $Yb_4Si_2O_7N_2$ (Yb), is shown in Fig. 3.9. The minimum strain rate of Lu48 at 1500 °C increases monotonically and that at 1400 °C increases slightly up to 250 MPa then rapidly above 250 MPa. The value of n is calculated assuming that the creep rate in the steady state is the minimum strain rate. The minimum strain rate of the fractured samples is used because the minimum strain rate obtained from interrupted test data may not be that of the steady state. The value of n for Lu48 is 6.8 at 1400 °C and 7.7 at 1500 °C. The value for Yb is 3.1 at 1300 °C, calculated from interrupted test data, and 1.7 at 1400 °C. Comparing Lu48 and Yb, Lu48 is more sensitive to stress than Yb [13].

Figure 3.10 shows the effect of the applied stress on the time to failure of Lu48 at 1400–1550 °C, together with the data for Yb and SN281, which denotes Lu_2O_3-containing silicon nitride produced by Kyocera [14]. The time to failure decreases with increasing applied stress. Comparing the data obtained at 1400 °C, the plots of Lu48 are much higher than those of Yb, meaning that Lu48 is more creep-resistant than Yb. The Lu48 data obtained at 1400 °C almost overlaps that of SN281 data
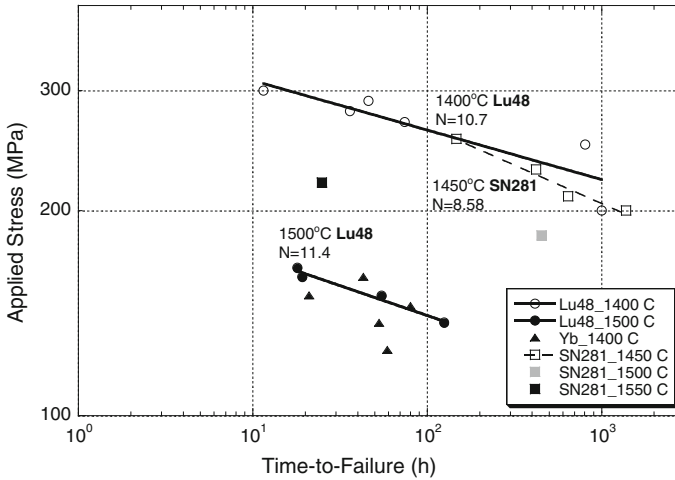
Fig. 3.10 Time to failure and applied stress for Lu48, Yb, and SN281 at 1400–1550 °C [12]

obtained at 1450 °C. Also, the Lu48 data obtained at 1500 °C is below the SN281 data obtained at 1500 and 1550 °C.

The time to failure t_f may be described as a power function of the stress σ:

$$t_f = B\sigma^{-N} \tag{3.2}$$

where N is a parameter describing the stress-rupture behavior. The value of N for Lu48 is 10.7 at 1400 °C and 11.1 at 1500 °C. The value for Yb was not calculated because of the large scattering of the data [15]. The value of N for SN281 is 8.58 at 1450 °C, which was obtained using the data in Ref. 14. Lu48 fractured at 1400 °C under a stress of 200 MPa after 1000.5 h, indicating that Lu48 can sustain creep for over 1000 h at 1400 °C under a stress of 137 MPa. Lu12 contains the smallest amount of additive among the ceramics investigated. The creep resistance of Lu12 was expected to be higher than that of Lu48. Lu12 sustained creep for 1678.5 h at 1500 °C under a stress of 137 MPa [14]. This result shows that Lu12 sustains creep for 1000 h at 1500 °C under a stress of 137 MPa, which is the goal of a project of National Institute for Materials Science (NIMS) for developing heat-resistant silicon nitride ceramics. The minimum strain rate could not be calculated because the displacement was below the minimum measurable value, particularly below 1500 °C.

The relationship between the applied stress and the time to failure is shown for Lu12 in Fig. 3.11. The time to failure tends to increase with decreasing applied stress. Plots are typically distributed from 0.08 to 228 h with a change in applied stress from 160 to 180 MPa at 1400 °C. At 1500 °C, the time to failure is distributed from 0.1 to 690 h with a change in applied stress from 145 to 165 MPa. The high sensitivity of the time to failure to the applied stress and the inability to detect deformation during creep tests suggest that the fracture of Lu12 is dominated by
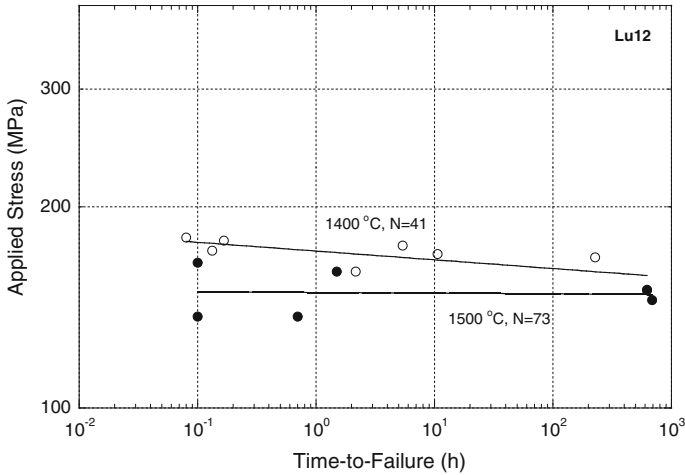
Fig. 3.11 Time to failure and applied stress for Lu12 at 1400 and 1500 °C [11]

subcritical crack growth, not creep rupture, particularly at 1400 °C. The stress-rupture parameter N is 41 at 1400 °C and 73 at 1500 °C, larger than the values for Lu48 (10.7 at 1400 °C and 11.1 at 1500 °C). The minimum strain rate of SN281 has been reported to be on the order of 10^{-10}–10^{-11} s^{-1} at 1400 °C and 10^{-9} s^{-1} at 1450 °C and above, much smaller than that of Lu48. No cavitation was detected in the creep specimens by transmission electron microscopy (TEM). A non-cavitation creep mechanism has previously been proposed [14]. Lu12 is not deformed by creep and is fractured by subcritical crack growth at 1400 °C. The characteristic features of Lu12 are its high sensitivity of the time to failure to the applied stress and its low fracture strength during subcritical crack growth. These features are not favorable as a structural material.

3.5 Conclusion

The use of grain boundary control to improve the heat resistance of silicon nitride ceramics was explained. The high-temperature properties of silicon nitride ceramics sintered with RE_2O_3 (RE: Yb and Lu), which were selected with the aim of achieving grain boundary control, were measured. The heat resistance of silicon nitride with Lu_2O_3 was greater than that of silicon nitride with Yb_2O_3 and SiO_2. The silicon nitride ceramic including a small amount of Lu_2O_3 (Lu12) had a lower strength at 1500 and 1600 °C than the silicon nitride ceramic with a large amount of Lu_2O_3 (Lu48). However, the creep resistance of Lu12 was higher than that of Lu48. These results suggest two important points. One is that a small amount of the grain boundary phase is more favorable for increasing heat resistance. Lu12 has lower

strength at 1500 and 1600 °C but its fracture was still brittle, its creep rate at 1400 and 1500 °C was too small to be detected, and its fracture during the tensile test might have been caused by, subcritical crack growth rather than creep. The oxidation resistance of Lu12 was higher than that of Lu48 [13]. When we consider densification, a certain amount of sintering additive is needed for complete densification. High-temperature properties, creep and oxidation resistance, are incompatible with sinterability from the viewpoint of sintering additives. The other point is that high-temperature strength is not always an indicator of heat resistance; although Lu12 had higher creep resistance than Lu48, Lu48 had higher high-temperature strength than Lu12. We must measure the creep to obtain information on heat resistance, considered here to be stability at a high temperature for a long time.

References

1. Gazza GE (1973) Hot-pressed Si_3N_4. J Am Ceram Soc 56:662
2. Hoffmann MJ (1994) Tailoring of mechanical properties of Si_3N_4 ceramics. In: Hoffmann MJ, Petzow G (eds) Kluwer Academic Publishers, Amsterdam, 1994, p 233
3. Nishimura T, Mitomo M (1995) J Mater Res 10:240
4. Tsuge A, Nishida K, Komatsu M (1975) J Am Ceram Soc 58:323–326
5. Wills RR, Stewart RW, Cunningham JA, Wimmer JM (1976) J Mater Sci 11:749
6. Hirosaki N, Yamamoto Y, Nishimura T, Mitomo M (2002) J Am Ceram Soc 85:2861–2863
7. Nishimura T, Mitomo M, Ishida A, Yoshida H, Ikuhara Y, Sakuma T (1997) In: Proceedings of 6th international symposium on ceramic materials and components for engines, pp 632–637
8. Cinibulk MK, Thomas G, Johnson SM (1992) Strength and creep behavior of rare-earth disilicate-silicon nitride ceramics. J Am Ceram Soc 75:2050–2055
9. Nishimura T, Mitomo M, Suematsu H (1997) J Mater Res 12:203–209
10. Smith JT, Quackenbush CL (1980) Am Ceram Soc Bull 59:529
11. Guo S, Hirosaki N, Yamamoto Y, Nishimura T, Kitami Y, Mitomo M (2003) Phil Mag Lett 83:357–365
12. Nishimura T, Hirosaki N, Yamamoto Y, Takigawa Y, Cao J (2005) J Mater Res 20:2213–2217
13. Nishimura T, Guo S, Hirosaki N, Mitomo M (2006) J Ceram Soc Jpn 114:880–887
14. Lofaj F, Wiederhorn SM, Long GG, Hockey BJ, Jemian PR, Browder L, Andreason J, Täffner U (2002) Non-cavitation tensile creep in Lu-doped silicon nitride. J Eur Ceram Soc 22:2479–2487
15. Cao J, Okada A, Hirosaki N (2002) Tensile creep behavior of an ytterbium silicon oxynitride-silicon nitride ceramic. J Eur Ceram Soc 22:769